DOI: 10.1002/ejoc.200500809

A Theoretical Study of the Stereoselectivities of the Diels–Alder Addition of Cyclopentadiene to Ethyl-(*S*)-lactyl Acrylate Catalyzed by Aluminium Chloride

Snezhana M. Bakalova[a,b] and A. Gil Santos*[a]

Keywords: Density functional calculations / Ab initio calculations / Chiral auxiliaries / Cycloaddition / Solvent effects

We have studied the $AlCl_3$-catalyzed cycloaddition of ethyl-(*S*)-lactyl acrylate (ELA) and cyclopentadiene (CPD) by MP2 and DFT (B3LYP) methods using the 6-31G(d,p) basis set, with or without solvent effects. Four types of dienophile–Lewis acid (LA) complexes were considered – two types of ELA·$AlCl_3$, ELA·2$AlCl_3$ and ELA·$AlCl_2^+$. The stereochemical predictions of these models were compared with available experimental data. The participation of lactate-bound ELA·$AlCl_3$ complexes is insignificant because of their relatively high TS energies. The diastereofacial selectivities exhibited by the chelated ELA·$AlCl_2^+$ complex do not agree with experimental data, suggesting that this type of complex is not very probable, even with ligands having an appropriate carbonyl orientation. Our results show the dominating role of ELA·2$AlCl_3$ in the catalyzed reaction, in agreement with experimental data. The observed diastereofacial stereoselectivities are due to a delicate equilibrium of electrostatic and steric interactions in the different transition states between the two LA groups and between these two groups and the cyclopentadiene moiety.

Introduction

Chiral auxiliaries are widely used as chemical blocks able to induce chirality into several known synthetic strategies.[1–3] Two interesting families of compounds, which have been used for more than 20 years, are oxazolidinones **1** and imidazolidinones **2**.[4–12]

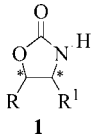
1

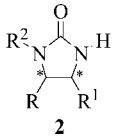
2

Oxazolidinones or imidazolidinones can be used as chiral auxiliaries in ionic,[10,13,14] radical[15–19] or even in dynamic kinetic resolution (DKR) reactions.[20–27] The majority of these reactions undergo acid catalysis and Evans and coworkers have proposed a mechanism to account for the reaction, as shown in Scheme 1.[5–8,11,12]

The "unexpected" stereochemistry, considering the steric effects of the ring substituent, can be understood by assuming that the reacting conformer is the one in which the two carbonyl groups are coplanar as a result of their complexation with the Lewis acid (Scheme 1).[12] Subsequently, it was assumed that this was the explanation for all reactions in which this stereochemistry was obtained (almost all cases). In the cases in which the "expected" stereochemistry was obtained, the explanation was always that no chelation took place with the attack from the less hindered face yielding the other possible epimer (Scheme 1).

Recently, we proposed an alternative mechanism to explain some of the observations in DKR reactions in which the stereochemistry can be explained in terms of the interactions between the leaving group and the attacking amine (Figure 1)[28,29] without any need for the high-energetic amide bond rotation. Based on this concept, we introduced small modifications into the chiral auxiliary[30] which maximized its performance in DKR reactions.

Considering the great importance of chiral auxiliaries based on oxazolidinone or imidazolidinone moieties, we are still engaged in improving the understanding of the mechanisms involved in all types of reactions in which these auxiliaries are used. Since many of the mechanisms proposed in the literature are based on the original mechanism proposed by Evans (Scheme 1), it became very important to us to decide on their validity since none of the many published papers is able to give a final answer to such an important and interesting problem.

The main problem we find when modelling the chelated complex is its ionic character, which makes it impossible to compare with the energy of the reagents or products. We know that the amide bond rotation is highly energetic and that the energy difference between the two extreme conformers is more than 7 kcal mol^{-1}.[29,30] This means that a larger energy stabilization, due to complex formation, is needed to shift the conformation from the *anti* to the parallel carbonyl orientation. Since we cannot theoretically eval-

[a] REQUIMTE-CQFB, Dep. Química, FCT, Univ. Nova Lisboa, 2829-516 Caparica, Portugal
[b] Institute of Organic Chemistry, Bulgarian Academy of Sciences, Acad. G. Bonchev str., block 9, 1113 Sofia, Bulgaria
E-mail: ags@dq.fct.unl.pt
Supporting information for this article is available on the WWW under http://www.eurjoc.org or from the author.

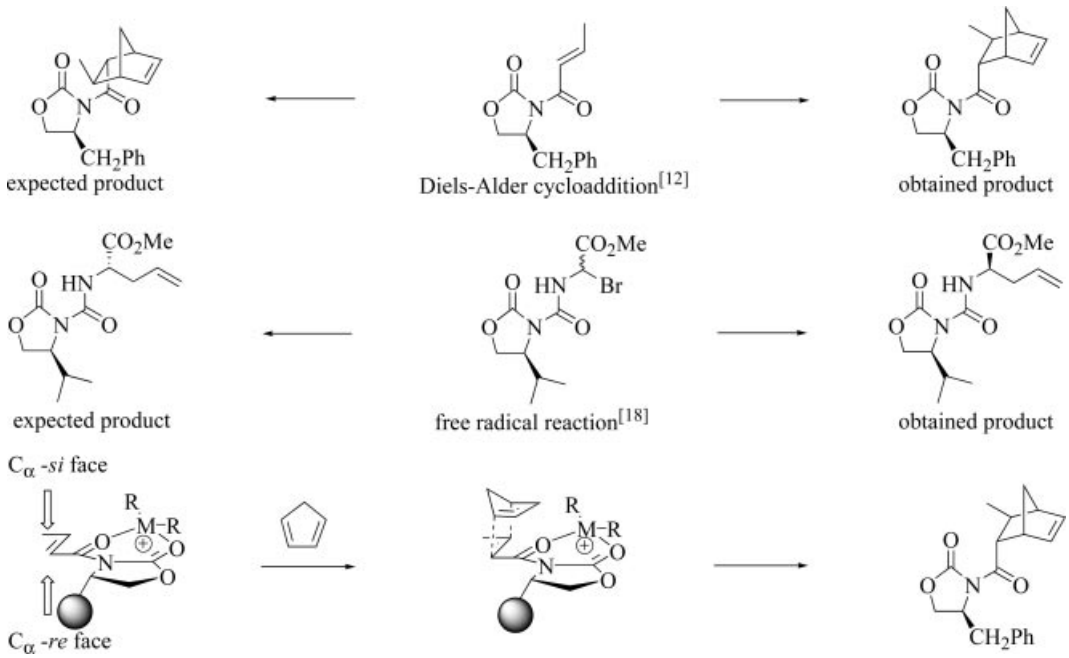

Scheme 1. Use of oxazolidinones as chiral auxiliaries in cycloaddition and free-radical reactions. Bottom: mechanism proposed by Evans et al.[12] to explain the results of their cycloaddition reactions.

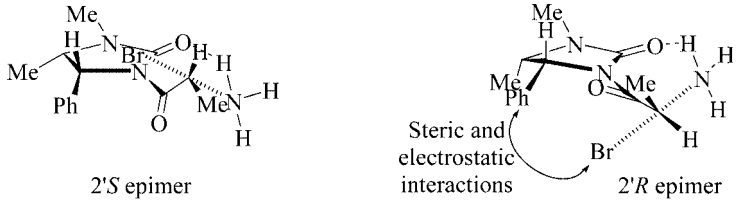

Figure 1. Reaction mechanism proposed by us as an alternative to Caddick's mechanism, based on theoretical results.[29,30]

uate such stabilization (ionic complex), we decided to look for a similar system, able to complex with aluminium salts, but having a parallel carbonyl conformer of low energy. If the Evans-type chelate formation lowers the energy relative to the open-chain complexes, then it should be formed since no substantial energy increase would occur due to a shift in the conformation.

Searching the literature we found that the chiral dienophile ethyl-(*S*)-lactyl acrylate [ELA, (*S*)-1-(ethoxycarbonyl)-ethyl acrylate] (**3**) and cyclopentadiene (CPD) undergo a stereoselective Diels–Alder (DA) cycloaddition reaction in the absence of a catalyst (Scheme 2).[31] The presence of two diastereotopic faces of different polarity in ELA ensures a reasonably high diastereoselectivity of up to 85:15. The moderate *endo*/*exo* selectivity is in the range of 1.68 (63:37) to 3.22 (76:24), being dependent on solvent polarity.[31] Our recent computational studies on this reaction[32] have reproduced the observed trends in both *endo*/*exo* and diastereofacial selectivities.

The Lewis acid (LA) catalysis of the same reaction leads to substantial improvements in the *endo*/*exo* selectivities of up to 32 (97:3).[31] Also interesting is the experimental observation that, depending on the LA, diastereofacial selectivities were inverted. In the cases of $BF_3{\cdot}Et_2O$, AlR_nCl_{3-n}

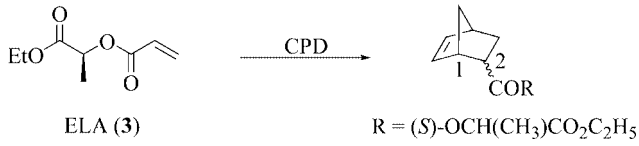

Scheme 2. Diels–Alder reaction of ELA and CPD.

and $ZrCl_4$, the (1*S*,2*S*) adducts (Scheme 3) were mostly formed, similar to the case of the uncatalyzed reaction. However, upon $TiCl_4$ or $SnCl_4$ catalysis, the preferred product has the inverse configuration.[31] Helmchen and coworkers suggested that the observed inversion is presumably due to the fact that the dienophile has two basic sites (carbonyl groups), enabling both mono- and bidentate complexation, changing the accessibility of the *re* and *si* faces.[31,33] This concept is, in all aspects, similar to the one proposed by Evans et al.[12] to explain the stereoselectivity observed in Diels–Alder reactions using dienophiles connected to oxazolidinone rings. In this paper we compare computational results on the stereoselectivity of the Diels–Alder cycloaddition of ELA and CPD catalyzed by aluminium trichloride obtained with different computational methods. A special emphasis is given to the stereoselective

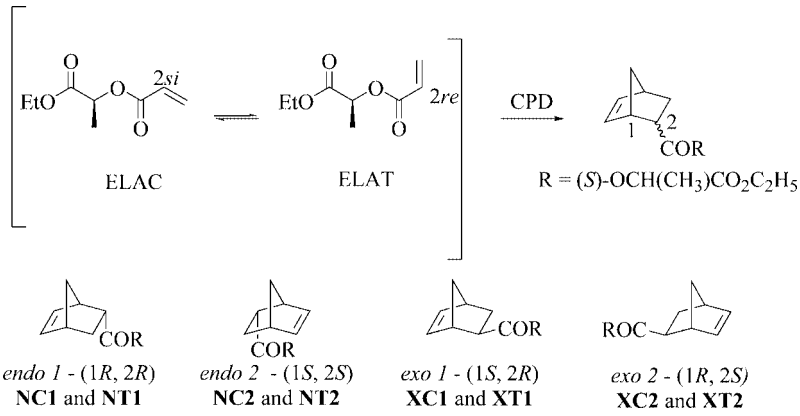

Scheme 3. Absolute stereochemical designations of reactants and products. The conjugated dienophile planes of ELAC and ELAT, respectively, coincide with the picture plane and the *si* and *re* diastereotopic faces face up, respectively.

performance of bis- and monometal cyclic complexes, aiming at establishing a direct comparison between this and Evans' auxiliary.

Computational Details

Full geometry optimizations were performed by employing MO theory[34] (MP2) or density functional theory (B3LYP[35]) with the 6-31G** basis set. All important structures were also calculated at the B3LYP/6-31G** level of theory with the Onsager solvation model using dichloromethane as solvent.[36,37] The medium-size 6-31G* basis set is usually considered sufficient for reliable optimization of geometries of reactants and transition structures in DA reactions. The polarization function on hydrogen atoms is included in the present study for a better description[38] of possible hydrogen bonding interactions involved in the DA mechanisms to be considered, thus enhancing the reliability of envisaged energy differences determining stereoselectivity. All calculations were carried out with the Gaussian 03 suite of programs[39] using default optimization criteria. Located B3LYP transition structures were verified by calculating the analytical vibrational frequencies, ensuring the presence of a unique imaginary frequency. Some of the transition structures were verified by IRC calculations[40] as well. Zero-point energies and thermal corrections were calculated from unscaled vibrational frequencies. Reported activation energies include the zero-point correction to energy. Activation free energies are given for 298.15 K. Reported stereoselectivity ratios were obtained by the summation of the calculated product percentages. Electronic surfaces were calculated using the Gaussian 03 package and displayed with GaussView 3.09.

Nomenclature Issues

The conformation of the acryloyl fragment of the dienophile is designated with **C** for *s-cis* and **T** for *s-trans*, respectively. Products are labelled in the traditional way,[41–43] with the corresponding reaction number and either **N**, for *endo* adducts, or **X**, for *exo* adducts, respectively. The absolute stereochemical designations of this nomenclature are given in Scheme 3. Cycloaddition transition-state structures are labelled according to the respective reaction product.

The chiral lactyl fragment of ELA is polar. Therefore, the diastereotopic faces of this dienophile are electrostatically nonequivalent. To distinguish between the two acrylate faces of ELA we refer to the face of COOEt as the polar one and to the face of H (CH_3) as the nonpolar one.

Results and Discussion

Ligand Coordination

As stated in the introduction, ELA has two ester carbonyl groups capable of binding LAs. For this reason, we consider four possible types of ELA·$AlCl_3$ complexes (Figure 2). Three of these exhibit monodentate coordination of Al to ELA, two with a molar ratio of 1:1 (monometal, **MA** and **ML**), and one with a molar ratio of 1:2 (bis-metal, **M2**) with a molecule of LA coordinated to each of the carbonyl oxygen atoms. We also consider the cyclic (bidentate) monometal complex of ELA (**MAL**) involving the cation $AlCl_2^+$, as originally proposed by Evans et al.[12] As explained in the introduction, we have a special interest in this type of complex since, in contrast to Evans' auxiliary, in the case

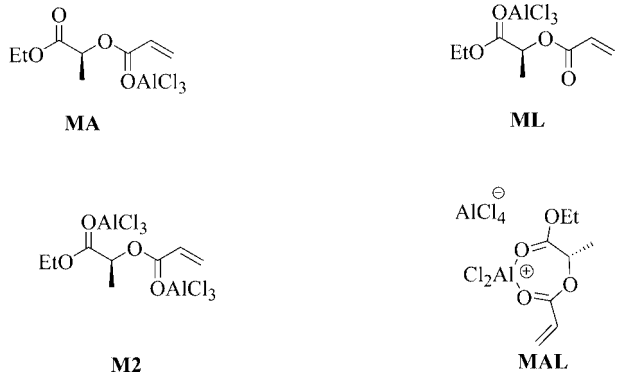

Figure 2. Aluminium chloride complexes of ELA in the *s-cis* conformation.

of ELA, it should be easily formed owing to the absence of strong energetic demands (less than 3 kcal mol^{-1} according to our conformational search). Nevertheless, based on the reaction's stereochemical outcome, Helmchen and co-workers suggest that this type of complex is not formed,[33] and the products obtained originate from complex **M2**.

Figure 3 shows the optimized structures of the most stable conformers of the complexes formed between ELA (*s-cis*, ELAC, and *s-trans*, ELAT) and $AlCl_3$. Our calculations predict stable 1:1 ELA·$AlCl_3$ complexes of comparable energy. The acrylate carbonyl oxygen of the dienophile is slightly more basic than the lactate one due to its α,β-conjugation with the double bond. Therefore, **MA** complexes are somewhat more stable than **ML** ones (Figure 3). In all complexes there are close Cl···H(C) contacts (nontraditional hydrogen bonds[37,44]) with the hydrogen atom at the asymmetric center of the chiral auxiliary and/or the vinyl hydrogen atom.

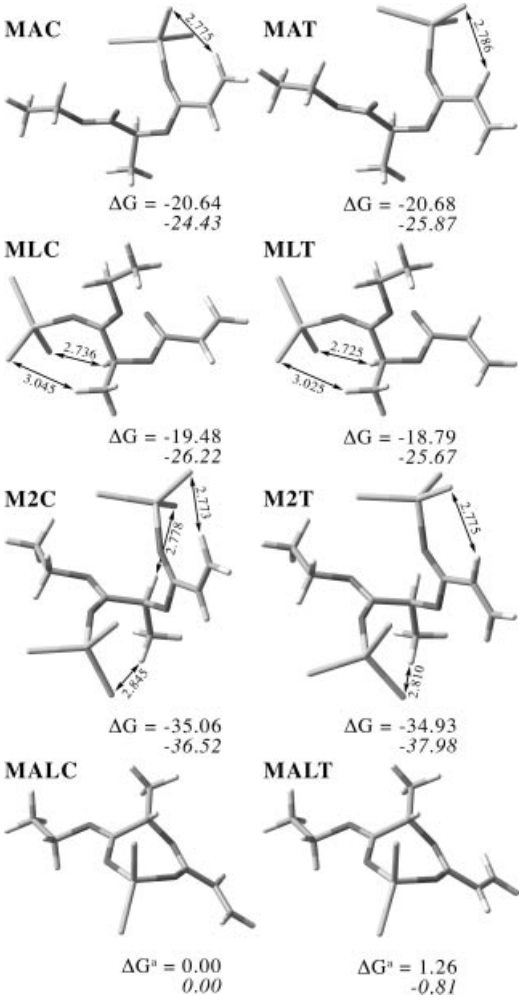

Figure 3. Structure, selected interatomic distances in Å (gas phase) and stabilization free energies (Δ*G*/kcal mol^{-1}) of ELA complexes with $AlCl_3$ determined at the B3LYP/6-31G** level of theory (Onsager values printed in *italics*). [a] Relative energies due to the ionic character of these complexes.

Coordination of a second LA molecule (**M2C** and **M2T**, Figure 3) brings about additional stabilization to the complexes, the energetic effect of the two coordination sites being almost additive. This result indicates that there are no specific electronic interactions between the two metal atoms via the organic ligand.

The number of possible complexes that can form between ELA and Lewis acids is further increased by the relatively free rotations around the single C–C and C–O bonds of the dienophile, as well as about the carbonyl–LA coordination bond(s), which results in small energy differences between the possible rotational isomers. The *s-cis*/*s-trans* conformational equilibrium of the acryloyl fragment of the studied dienophile is of special importance to the analysis of its enantioselective reactions since the interconversion of the two conformers results in the interchange of the *re* and *si* faces of the dienophile (Scheme 3). The *s-cis* isomer of ELA, ELAC, is more stable than the *s-trans*, ELAT, as observed in other acrylates, but unlike other unsaturated carbonyl compounds.[45] The free-energy difference between ELAC and ELAT is about 0.5 kcal mol^{-1},[32] while the electronic energy barrier to the internal rotation about the C–C single bond is 7 kcal mol^{-1}, similar to the values found for acrylic acid and methyl methacrylate (ca. 8 kcal mol^{-1}).[45,46] In the lactate monocomplexes (**ML**) this energy difference remains similar. In the acryloyl monocomplexes (**MA**), however, as well as in the 2:1 complexes (**M2**), the *s-cis* conformers are practically isoenergetic with the *s-trans* ones, without any significant change in the activation free energy for interconversion. Consequently, coordination of an $AlCl_3$ molecule to the acrylate carbonyl group of ELA shifts the *s-cis*/*s-trans* equilibrium towards the *s-trans* conformer, as previously found for other chiral acrylates. As expected, **MAL**-type complexes do not exhibit this behavior, since the LA moiety is far from the enolate group, the energy difference between the two conformers being more than 1 kcal mol^{-1}.

Solvent effects, in spite of having an important effect on the relative energies, do not reveal major structural changes. The main contacts remain, with small corrections to the contact distances. As expected, for the acryloyl complexes the contribution of *s-trans* conformers substantially increases due to their larger dipole moment, being considerably more stable than the *s-cis* ones.

Reactivity

The original work of Helmchen and co-workers[31] is limited to the study of LA concentrations up to 1.1 equiv. In their second paper[33] this limit was increased up to 2.5 equiv. The main problem we face when analyzing these two papers is that almost all the useful data regarding stereoselectivity is obtained from the first one. The second one only gives information on diastereofaciality. Since, according to the results of Helmchen and co-workers, with 1 equiv. of LA the reaction has to proceed through complex **MA** and, with more than 2 equiv. of LA, through complex **M2**, one has to be specially careful when comparing theoretical data with his experimental values. Effectively, com-

Table 1. Experimental[31] and computed (B3LYP/6-31G**) product stereoselectivity ratios for the DA reaction between ELA and CPD.[a]

Selectivity	Noncatalyzed Calcd.[b][32]	Exp.[c][31]	Calcd.[d],[32]	Exp.[e][31]	Catalyzed Calcd.[b] **MA**	Calcd.[b] **M2**[f]	Calcd.[b] **M2**	Calcd.[b] **MAL**	Calcd.[d] **MAL**	Exp.[f]
endo/*exo*	28:72	63:37	63:37	76:24	65:35	84:16	68:32	56:44	60:40	93:7[31]
endo 1/*endo 2*	15:85	20:80	11:89	42:58	20:80	14:86	3:97	81:19	78:22	36:64[31] (22:78)[g]
exo 1/*exo 2*	11:89	15:85	28:72	32:68	42:58	40:60	9:93	82:18	69:31	–

[a] All selectivities include the contribution of the eight possible transition states. [b] Gas phase. [c] Hexane, 273 K. [d] CH_2Cl_2, 298 K. [e] CH_2Cl_2, 273 K. [f] CH_2Cl_2, 228 K. [g] CH_2Cl_2, 209 K, 2.5 equiv. of CH_3AlCl_2.[33]

plexes **MA** and **ML** have to be compared with experimental results for 1.1 equiv. of LA,[31] while complexes **M2** and **MAL** have to be compared with experimental results obtained with 2.5 equiv. of LA.[33] Another point which has to be considered is that while our study was made with only aluminium trichloride, in their second paper Helmchen and co-workers used ethylaluminium dichloride. Nevertheless, we believe that this difference will not affect the results much.

We first present and discuss the results of calculations at the B3LYP/6-31G** level of theory (Table 1, Figure 4) as this functional has been shown to predict, in many cases, exceptionally well the activation parameters and stereoselectivities of DA reactions. However, considering the high asynchronicity predicted by the B3LYP/6-31G** calculations, we also consider minimizations at the MP2/6-31G** level of theory in order to decide between a concerted and a two-step mechanism.

Table 1 allows a comparison between calculated (B3LYP/6-31G**) and experimentally observed selectivities, with or without solvent effects.

The results from the B3LYP computational model of DA addition of ELA·$AlCl_3$ to CPD, with coordination of $AlCl_3$ to the lactate oxygen atom of ELA (**MLC**, Figure 3), are not given in Table 1 as, although the complexes **MA** (at the acrylate oxygen atom) and **ML** (at the lactate oxygen atom) are of similar energy (Figure 3), the TSs derived from the latter have significantly higher energies (ca. 7 kcal mol^{-1}) than the ones derived from the acrylate complexes, as a result of the absence of conjugation to the acrylate double bond. This prediction obviously renders the participation of lactate-bound LA complexes of ELA insignificant in the catalytic reaction considered.

Let us start our discussion with the gas-phase values. A feature of immediate interest in the reaction proceeding via **MA** complexes at the B3LYP/6-31G** level of theory is the increased asynchronicity of the catalyzed cycloaddition relative to the uncatalyzed one. While the asynchronicity ratio $d2/d1$ ($d1$ and $d2$ are the lengths of the forming bonds) for the uncatalyzed addition of ELA to CPD is about 1.20, LA catalysis by a single $AlCl_3$ molecule leads to an increase in this value to about 1.35–1.40. This finding is consistent with the expected increased asynchronicity of the DA reaction under LA catalysis[47] due to the increased polarization of the dienophile double bond. The calculated product percentages indicate an increased contribution of the *s-trans* TSs and their respective products in the catalyzed reaction

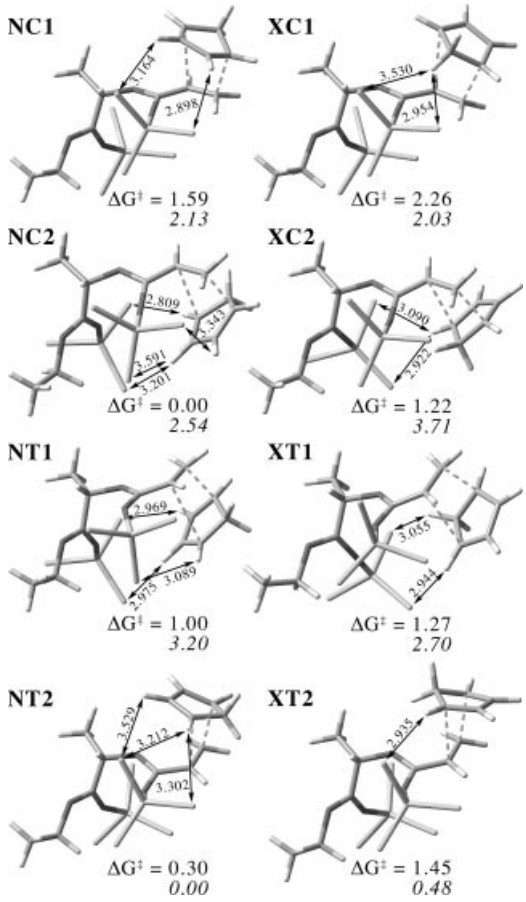

Figure 4. Transition-state structures for the DA addition of ELA·2$AlCl_3$ (**M2C** and **M2T**) to CPD determined at the B3LYP/6-31G** level of theory. Relative activation free energies with respect to **NC2** (gas phase) or **NT2** (solvent; values printed in *italics*) are given in kcal mol^{-1}. Close contacts (nontraditional hydrogen bonds) between the diene and the LAs shorter than 3.6 Å are included (calculated in the gas phase).

(ca. 33%) relative to the uncatalyzed case (ca. 3%),[32] which results mainly from the increased contribution of **NT1** (ca. 12%) and **XT1** (ca. 14%).

The calculated activation energies of the studied DA addition, catalyzed by a single $AlCl_3$ molecule coordinated to the acrylate carbonyl group, are lower by more than 10 kcal mol^{-1} than those obtained for the uncatalyzed reaction. Earlier theoretical work on LA catalysis of the DA reaction of acrolein and butadiene[41] showed approximately the same reduction in the activation parameters with either BF_3 or $AlCl_3$ (ca. 9–10 kcal mol^{-1}).

Compared with the known experimental data on the $AlCl_3$-catalyzed addition of ELA to CPD, with a 1.1:1 ratio of Lewis acid to ELA,[31] our B3LYP/6-31G** computational results with **MA** as dienophile show underestimated *endo*/*exo* selectivity (see Table 1). Comparison of calculated product stereoselectivities for catalyzed versus uncatalyzed addition of ELA to CPD (Table 1) shows, in disagreement with experiment, decreased *endo* diastereofacial ratios under catalysis. Even so, the theoretical prevision still overestimates the experimental results. Summarizing, computations involving **MA** as dienophile underestimate the *endo*/*exo* ratio and slightly overestimate the diastereofacial selectivity.

Let us consider now the catalyzed addition of ELA to CPD via a 2:1 complex, with a molecule of $AlCl_3$ coordinated to each carbonyl group of the dienophile (**M2**). The transition-state structures of this DA reaction, together with the relative activation free energies, are shown in Figure 4.

Complexation of a second LA molecule to the lactate oxygen of ELA leads to a further reduction in the activation energies by about 1–2 kcal mol^{-1} relative to the **MA** reaction. This decrease is comparable to the one calculated for the **MLC** reaction relative to the uncatalyzed case (ca. 3 kcal mol^{-1}), that is, the effect of $AlCl_3$ coordination to the two carbonyl groups on the TS energies is approximately additive, similar to the case of the above discussed relative stabilization of the dienophile–$AlCl_3$ complexes. However, more interesting are the stereoselectivity changes brought about by the second coordination. As is evident from the calculated product percentage ratios, the complexation of a second $AlCl_3$ molecule to ELA increases both the *endo*/*exo* and diastereofacial (**N2** vs. **N1**) selectivities, while the *exo* diastereofacial (**X2** vs. **X1**) selectivity remains practically unchanged (Table 1). The computational prediction of a moderate enhancement of the *endo* diastereofacial (**N2** vs. **N1**) selectivity in the DA cycloaddition that proceeds via complex **M2** relative to the uncatalyzed case is in agreement with the experimentally observed trend upon catalysis in CH_2Cl_2 (Table 1, columns 5 and 9). If one compares the calculated selectivity ratio with that experimentally observed, quite a good agreement can be found for a LA concentration of 2.5 equiv.

The predicted total *endo*/*exo* ratio for ELA·2$AlCl_3$ addition to CPD is about 84:16, also correctly reproducing the experimentally (Table 1, columns 5 and 11) observed trend of increase upon catalysis. The underestimated theoretical value shows similar behavior to that previously observed for the uncatalyzed reaction,[32] which confirms our previous conclusion of the poor performance of B3LYP for predicting *endo*/*exo* ratios. The correct prediction of stereoselectivity trends upon LA catalysis via **M2** may be considered an indication of the major role of the doubly metal-coordinated dienophile in the actual reaction for high concentrations of LA. Nevertheless, considering the nonexistence of experimental *endo*/*exo* ratios for LA concentrations over 1.1 equiv., the participation of **MA** complexes in the overall reaction, for such concentrations, cannot be completely ruled out based only on the theoretical predictions.

The relative contribution (ca. 45%) of the *s-trans* TS is also increased in the 2:1 complexes, largely due to the significantly enhanced contribution of **NT2** (ca. 27%).

The experimental results[31,33] strongly support the thesis of major participation of double-complex transition states. Nevertheless, a stoichiometry of LA/ELA of 2:1 does not allow for a distinction between **M2** or **MAL**. Helmchen and co-workers circumvented this problem, comparing the behavior of the aluminium catalysts with the titanium ones. Assuming that they should be similar, it was argued that while titanium can form chelates of **MAL** type, depending on LA concentration, aluminium catalysts only form complexes of **MA** and **M2** types. While this argument is acceptable, we need to have stronger ones if we want to extrapolate to other systems. With this in mind, we consider the catalysis of ELA addition to CPD via chelate-type complexes with aluminium chloride (**MAL**, Figure 2). The predicted product distributions determined by B3LYP/6-31G** calculations are given in Table 1, while the TSs and their relative activation free energies are shown in Figure 5.

Comparison of stereochemical predictions for the cyclic ELA·$AlCl_2^+$ model and reported experimental data (Table 1) unambiguously shows that the chelated model does not agree with the experimental data regarding diastereofacial selectivity. In fact, the prediction of an *endo 1*/*endo 2* ratio of 81:19 is opposite to the experimental preference of 22:78. The prediction of an *endo*/*exo* ratio of 56:44, even if it should not be considered too literally, is also quite different from the experimental 93:7, also suggesting that this type of complex should not be involved in the studied reaction.

The inclusion of solvent effects does not change the above conclusion. Solvent effects slightly decrease the *endo*/*exo* ratio, but substantially increase the diastereofacial selectivity of the **M2** transition states. On the other hand, there are no major changes when considering **MAL** transition states.

Mechanistic Aspects

The most asynchronous TSs for ELA addition to CPD are found for the ELA·2$AlCl_3$ complexes (Figure 4) and the cyclic ELA·$AlCl_2^+$-chelated complexes (Figure 5) with computed asynchronicity ratios ($d2/d1$) approaching 1.5 at the B3LYP/6-31G** level of theory. Full B3LYP/6-31G** IRC calculations of the lowest-energy TS geometry with ELA·2$AlCl_3$ (**NC2**, Figure 4) show the reaction to be concerted. Although the IRC profile obtained has a shoulder on the product side and some instability of the DFT solution in this region is clearly apparent (in the form of erratically changing optimization directions), all attempts to optimize an intermediate in the region of the shoulder failed and led to the product. In the case of the cyclic ELA·$AlCl_2^+$ complex, the IRC calculations performed at the B3LYP/6-31G** level of theory, starting from the lowest-energy TS (**NC1**, Figure 5), also indicate concertedness of the reaction when calculated in the gas phase.

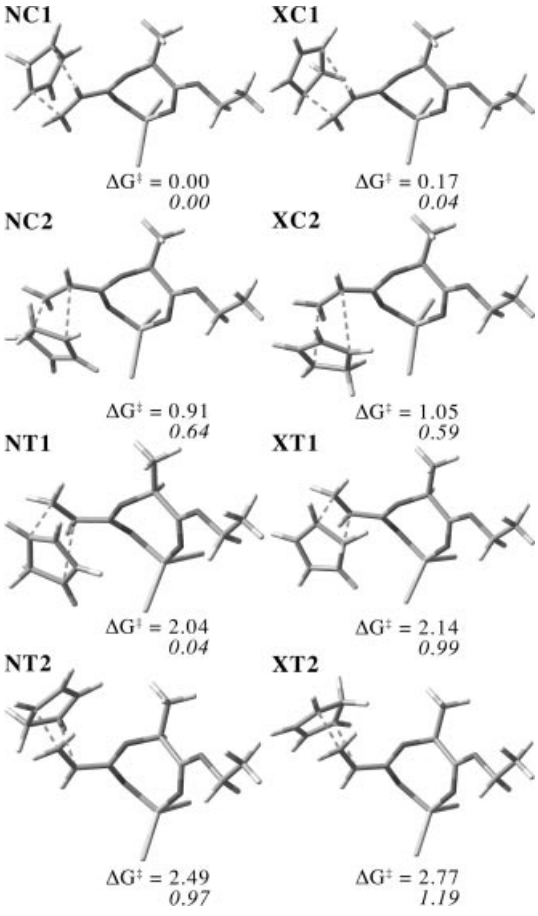

Figure 5. Transition-state structures for the addition of ELA·$AlCl_2^+$ (**MALC** and **MALT**) to CPD determined at the B3LYP/6-31G** level of theory. Relative activation free energies with respect to **NC1** are given in kcal mol^{-1}. Results obtained with the solvent model are printed in *italics*.

Transition-state optimizations with the Onsager solvent model show a slight increase in the asynchronicity of some structures. This means that, at this level of theory, we are at the border between a concerted and a two-step mechanism. To further ensure our confidence in the concertedness of the reaction, we performed complete geometry optimizations of some representative TSs of both complexes − ELA·2$AlCl_3$ and ELA·$AlCl_2^+$ − at the MP2/6-31G** level of theory. Not surprisingly, MO calculations predict significantly more synchronous structures than DFT, with *d*2/*d*1 lower than 1.2, which may be considered a very decisive argument in favor of the concerted DA addition of ELA to CPD upon $AlCl_3$ catalysis. This prediction is in agreement with the experimental results and theoretical predictions for similar systems.[48] This means that one has to be careful when modeling DA transition states, using DFT theory, with strongly polarized dienophiles.

Origins of Stereoselectivity

Searching the literature, we can conclude that, still today, there is a strong debate around the phenomena conditioning *endo*/*exo* selectivity.[38,49,50] Our own attempts to understand these phenomena brought us to the conclusion that it is still necessary to carry out more in-depth studies on a variety of simpler systems if we want to understand complex ones as that discussed in this paper. Electronic, electrostatic and steric effects are all important factors and it is our understanding that it would not be correct to attempt to justify this kind of selectivity based only on one of these factors. These conclusions, together with the observation of the poor performance of the B3LYP computational model, the main theory used in this work, do not allow us to discuss *endo*/*exo* selectivity in any depth. Nevertheless, by considering only the diastereofacial selectivity, we believe that a few conclusions can be drawn, especially when comparing the behavior of **M2** and **MAL**.

The origin of diastereofacial selectivity in the uncatalyzed reaction is mainly electrostatic and arises from weak stabilizing CH···O=C interactions between the diene and the dienophile moieties in the energetically favoured TSs.[32] The addition of a single molecule of $AlCl_3$ preferentially affords the complex at the acrylate oxygen atom. This complexation strongly increases the reactivity of the double bond, lowering the transition-state energy by about 10 kcal mol^{-1}, as already reported. The accepted justification for this difference relies on the lowering of the LUMO energy of the dienophile, but we can also see that electrostatic effects have to be considered since the attacking diene can establish one or more close contacts between its hydrogen atoms and the chlorine atoms in the Lewis acid (Figure 6).

Experimental data show that complexation with a single molecule of $AlCl_3$ does not seem to affect the diastereofacial selectivity much, while considerably increasing the *endo*/*exo* selectivity. Complexation with a second molecule of LA substantially increases the diastereofacial selectivity, while no data has been published for the *endo*/*exo* ratio. Our calculations do not reflect this observation, as can be seen in Table 1. Very similar diastereofacial values were obtained for noncatalyzed and catalyzed systems that proceed through **MA** or **M2**. Nevertheless, if we think that the TS energy of the highest experimentally observed diastereofacial selectivity is only around 1 kcal mol^{-1} more than that of the lowest observed selectivity and that this difference is derived from the relative energies of four TS structures, the theoretical error becomes easily acceptable. This statement makes even more sense if the reaction is strongly dependent on solvent effects, as has been shown experimentally.[31,33] Even considering these limitations, if we compare the noncatalyzed and the catalyzed TSs, interesting conclusions can be reached.

Comparison of the *endo* transition states reveals two main differences between those resulting from the bis-complexes **M2** (Figure 4), the monocomplexes (**MA**) or the uncatalyzed systems (Figure 6). The first difference regards the higher probability of complexed *s-trans* transition states. The second difference is the order of increasing energy, being **NC2**<**NC1**<**NT1**<**NT2** for the uncatalyzed TSs, **NC2**<**NT1**<**NT2**<**NC1** for **MA** TSs and

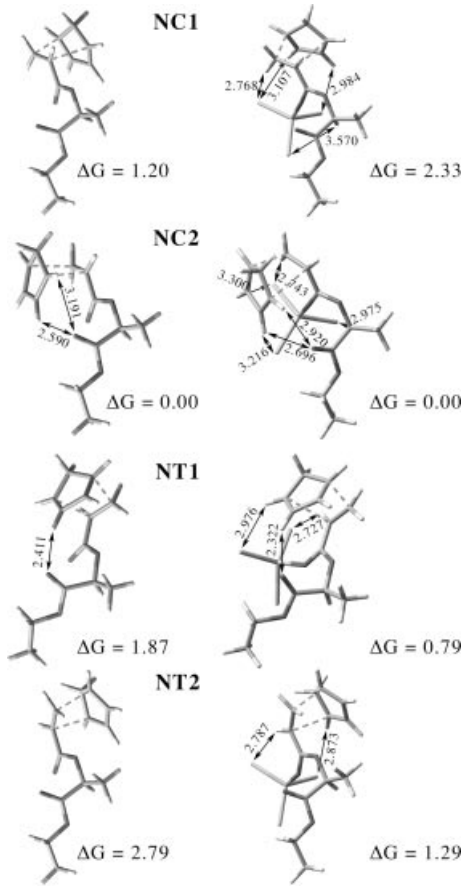

Figure 6. *endo* transition-state structures for the DA addition of ELA and ELA·$AlCl_3$ to CPD determined at the B3LYP/6-31G** level of theory. Relative gas phase activation free energies with respect to **NC2** are given in kcal mol^{-1}. Close contacts (nontraditional hydrogen bonds) between the diene and the dienophile or the LAs shorter than 3.6 Å are included.

NC2<**NT2**<**NT1**<**NC1** for **M2** TSs. This means that while in the uncomplexed and the **MA** systems the attack from the polar face is always less energetic than the attack from the nonpolar face, in **M2** *s-trans* the opposite is true. These differences seem to be a result of a delicate equilibrium between steric repulsive and electrostatic attractive forces between the diene hydrogen atoms and the chlorine atoms of the LA.

If one compares the complexes **MAC** with **MAT** and **M2C** with **M2T** (Figure 3), it is easy to conclude that the distance between the reactive double bond and the acrylate LA is larger in the *s-trans* conformers. This is the main reason why the complexation with a molecule of the LA attached to the acrylate carbonyl group shifts the *s-cis*/*s-trans* equilibrium to the *s-trans* side. When the CPD attacks the double bond, the acrylate LA moves to get the best interaction with the attacking group, reaching a position in one or the other face of the double bond in order to reduce the steric repulsion and keep the electrostatic attraction at a maximum (Figure 4 and Figure 6). As we said in the introduction, ELA has two faces of different polarity as a result of the carboxy moiety. When the acrylate LA moves in the direction of the ELA's polar group, the electrostatic repulsion increases, forcing an increase in the steric repulsion between the CPD ring and the acrylate LA. This is the main reason why the energy difference between **MA–NC1** and **MA–NC2** (Figure 6) increases compared with the uncatalyzed system. The average distance between the CPD hydrogen atoms and the LA is shorter in **MA–NC1**, meaning stronger steric repulsion. In the *s-trans* structures a similar situation exists, but with smaller and opposite results. This is because, while in the *s-cis* structures the LA lies on the opposite face to that of the attacking diene, in the *s-trans* structures both groups lie on the same face of the dienophile (reduction of the steric repulsion and electrostatic attraction at a maximum). The result of this is that when CPD attacks the double bond in **MA–NC1**, the LA group is forced inside the polar and more crowded concavity. In **MA–NT2** the CPD attack forces the LA group to move outside of this concavity, slightly reducing the steric and electrostatic repulsions. The final result is that, while the energy difference between the *s-cis* TSs increases on going from the uncatalyzed to the **MA** structures, the opposite is observed for the *s-trans* TSs.

When introducing a second LA molecule, the LA–carboxy-group repulsion is replaced by LA–LA repulsion, with a similar result to that discussed above. On the other hand, the system has another source of steric repulsion with the attacking CPD. The main result is that structures **M2–NC2** and **M2–NT1** (attack from the polar face, Figure 4) are less stabilized. The energy difference between the two *s-cis* structures is now only 1.6 kcal mol^{-1}, the energy difference between the two *s-trans* structures being inverted, with **M2–NT2** more stable than **M2–NT1**. The destabilizing factors are, in **M2–NC1**, the steric repulsion between the CPD ring and the acrylate LA and the electrostatic repulsion between the two LA moieties (Figure 7). In **M2–NC2**, the main destabilizing factor is the steric repulsion between each of the LA groups and the CPD ring due to its position on the crowded face. Nevertheless, **M2–NC2** is still relatively more stable (but not as much as **MA–NC2**) due to positive electrostatic attractions between the CPD ring and the two LA groups. In **M2–NT1**, the steric repulsion between the CPD ring and the LA groups plus the electrostatic repulsion between the two LA moieties (Figure 7) overcomes the electrostatic attractions between the CPD ring and the LA groups, rendering this TS more unstable than **M2–NT2**. This last structure is the one that "feels" the destabilizing phenomena least, having a very similar energy to that of **M2–NC2**.

The above analysis becomes very important when trying to rationalize the calculated results for **MAL** complexes. As we said in the introduction, the main objective of this work was to evaluate the probability of formation of chelates with bidentate ligands when aluminium salts are used. Considering the conformation of the free ligand (ELA) in which the two carbonyl groups have a suitable orientation to form cyclic complexes, ELA should have a high probability of forming such types of complexes, as long as the LA allows it.

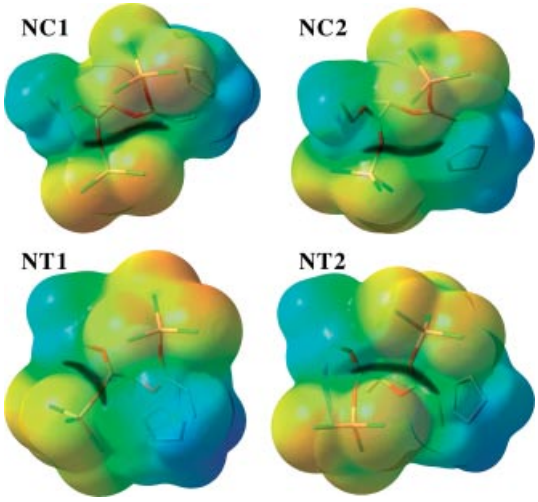

Figure 7. Electronic isodensity surfaces mapped with the electrostatic potentials (0.0004 $e^{-1}au^{-3}$) of selected TSs in the DA addition of CPD to ELA·2$AlCl_3$. Repulsive electrostatic contacts between the two LA moieties are marked in black.

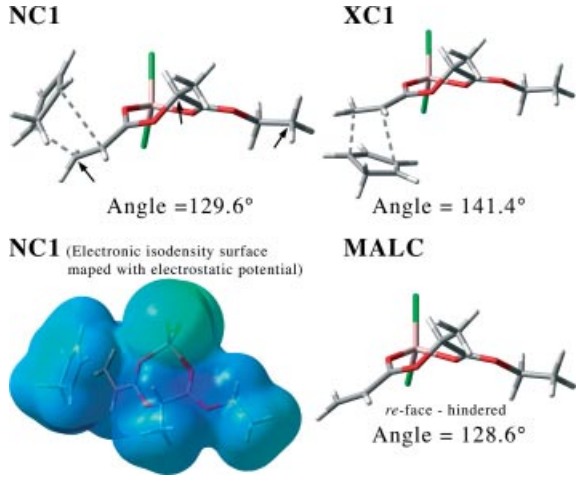

Figure 8. ELAC·$AlCl_2^+$ and selected TSs (gas phase) for its addition to CPD determined at the B3LYP/6-31G** level of theory. Ring-distortion angles are defined by the terminal atoms of the hydrocarbon chains and the chiral carbon atom in the chelate ring itself. Electronic isodensity surface as in Figure 7.

The values shown in Table 1 predict inverse diastereofacial selectivity to that experimentally observed. Considering that the two diastereofacial predictions for **M2** and **MAL** are separated by more than 2 kcal mol^{-1}, we can be quite confident that the chelated form will not have an important role in the reaction mechanism. The theoretical stereochemical outcome of the chelated TSs (Figure 5) is a result of the additional positive charge on aluminium, which significantly reduces the electrostatic stabilization caused by hydrogen-bond formation with the chlorine atoms (see the electronic surface in Figure 8). Also, since the lactyl carbonyl group is not free to interact with the attacking diene, steric requirements seem to dominate the predicted diastereofacial selectivity of the cyclic dienophile–LA complex. The attack on the *re* face, relative to the α-acrylate carbon atom of the dienophile is accompanied by dienophile distortion (Figure 8) as this concave face is sterically hindered. No such distortion is necessary upon attack on its convex *si* face, thus originating the calculated energy difference.

Solvent effects fully confirm our interpretation of steric and electrostatic interactions in the gas phase. In the case of **M2** complexes (Figure 4), **NT2** and **XT2** contribute, in dichloromethane, more than 95% to the overall diastereofacial selectivity. Any diene attack on the polar face (**NC2**, **XC2**, **NT1** and **XT1**) is of relatively high energy since electrostatic attractions are minimized, while steric effects, being very important in such TSs, dictate the final calculated energies. Also, the high energies calculated for **NC1** and **XC1** with the solvent model, show that, in agreement with our previous discussion, *s-cis* structures are too crowded to properly accommodate the attacking diene and the acrylate LA. In spite of large differences in the relative energies, the inclusion of solvent did not substantially change any of the calculated transition states, with only small changes to reaction asynchronicity and minimal adjustments to the lengths of the electrostatic contacts.

The results obtained for **MAL** transition states (Figure 5) also confirm the previous discussion. In this case, since electrostatic attraction has a minimal contribution to the overall energy in any of the eight TSs, the inclusion of solvent only contributes to an increase of the *s-trans* conformations, as expected. Both the diastereofacial selectivity and the *endo*/*exo* relation remain very similar to the gas-phase values, also suggesting that chelated transition states shall not be involved in the reaction mechanism.

Note that our general predictions are in full agreement with the results of Helmchen and co-workers and with their suggested mechanisms. In fact, they suggest that chelated complexes should not exist since this would decrease the diastereofacial selectivity, by comparison with the titanium behavior. Since titanium or aluminium chelates are chemically quite different (aluminium chelates need a counterion to neutralize the positive charge[12]), we have to consider some different scenarios. If the chelate is more stable than any other complex, then as soon as one adds some amount of aluminium salt to the reaction, the diastereofacial selectivity should be reduced. At higher concentrations the diastereofacial selectivity should finally be inverted giving high values; *endo*/*exo* selectivity, according to our calculations, should never be high. If the acrylate monocomplex has a higher stability than the chelate, then initially one should observe an improvement in the diastereofacial selectivity and, as soon as the chelate started to form, a decrease should be observed, finally leading to inversion of the configuration; *endo*/*exo* selectivity should initially increase and, finally, should be reduced to near 1. A scenario involving the coexistence of several complex types is also possible but, in such a situation, to account for the observed experimental diastereofacial selectivity and also the *endo*/*exo* relation, the amount of chelated complex has to be very low and the reaction can be considered as proceeding through **M2** or a mixture of **M2** and **MA**. In any case, **MAL**-type complexes should not be considered since they would always give a

diastereofacial selectivity/concentration chart opposite to that of Helmchen and co-workers.[33]

The interesting conclusion drawn from the above discussion is that if chelated complexes are not formed with ligands of low energetic demands, they should also not be formed with ligands that demand high energy for conformational change. If this is true, then the mechanisms proposed by Evans et al. and extensively used thereafter[12,51–53] may need a different analysis and, perhaps, a few adjustments. We aim to contribute, in the near future, further work in this field.

Conclusions

DFT and MO computational results are presented for the $AlCl_3$-catalyzed DA addition of ELA to CPD via four types of ELA·LA complexes − two types of ELA·$AlCl_3$, ELA·2$AlCl_3$ and ELA·$AlCl_2^+$. Verification of mechanistic and energetic results supplied by the discussed computational models is provided by comparison of their respective stereochemical predictions with available experimental data. Our results (both activation parameters and diastereoselectivity ratios) show the dominating role of the doubly metal-coordinated dienophile, ELA·2$AlCl_3$, in the catalyzed reaction. The observed diastereofacial selectivity is mainly a result of the electrostatic and steric repulsions between the two LA moieties, which fully agree with the results obtained using solvation models. These interactions force the TS structures to exist as very hindered conformations in which a delicate equilibrium between electrostatic and steric effects between the CPD hydrogen atoms and the chlorine atoms of the LAs dictates the final calculated selectivities. In the absence of a second LA molecule (**MA** structures), the scenario changes considerably with the system becoming more similar to the uncatalyzed one. When considering solvent effects, the system becomes simpler, with only two *s-trans* transition states being responsible for the observed stereoselectivity.

The computational predictions for the bidentate model, ELA·$AlCl_2^+$, find no support from the experimental results. Therefore, we are left to conclude that the DA additions of ELA complexes with aluminium salts to dienes do not involve chelates. The calculation of the TS structures at the MP2/6-31G** level of theory confirms the proposal of a concerted mechanism.

Supporting Information: Tables with B3LYP results, B3LYP and MP2 Cartesian coordinates and total energies of transition structures.

Acknowledgments

The financial support of the FCT, Portugal, FEDER (Ref. POCTI/QUI/42983/2001 and Ref. SFRH/BPD/11523/2002) is gratefully acknowledged.

[1] I. Suzuki, H. Kin, Y. Yamamoto, *J. Am. Chem. Soc.* **1993**, *115*, 10139–10146.
[2] P. Camps, F. Pérez, N. Soldevilla, *Tetrahedron: Asymmetry* **1997**, *8*, 1877–1894.
[3] V. J. Blazis, K. J. Koeller, C. D. Spilling, *J. Org. Chem.* **1995**, *60*, 931–937.
[4] H. Roder, G. Helmchen, E.-M. Peters, K. Peters, H.-G. Schnering, *Angew. Chem.* **1984**, *96*, 895–896; *Angew. Chem. Int. Ed. Engl.* **1984**, *23*, 898–899.
[5] D. A. Evans, J. Bartroli, T. L. Shih, *J. Am. Chem. Soc.* **1981**, *103*, 2127–2129.
[6] D. A. Evans, M. D. Ennis, D. J. Mathre, *J. Am. Chem. Soc.* **1982**, *104*, 1737–1739.
[7] D. A. Evans, *Aldrichimica Acta* **1982**, *15*, 23–32.
[8] D. A. Evans, M. M. Morrissey, R. L. Dorow, *J. Am. Chem. Soc.* **1985**, *107*, 4346–4348.
[9] I. Abrahams, M. Motevalli, A. J. Robinson, P. B. Wyatt, *Tetrahedron* **1994**, *50*, 12755–12772.
[10] A. Abdel-Magid, L. N. Pridgen, D. S. Eggleston, I. Lantos, *J. Am. Chem. Soc.* **1986**, *108*, 4595–4602.
[11] D. A. Evans, A. E. Weber, *J. Am. Chem. Soc.* **1986**, *108*, 6757–6761.
[12] D. A. Evans, K. T. Chapman, J. Bisaba, *J. Am. Chem. Soc.* **1988**, *110*, 1238–1256.
[13] G. Cardillo, L. Gentilucci, M. Gianotti, A. Tolomelli, *Org. Lett.* **2001**, *3*, 1165–1167.
[14] K. J. Hale, J. Cai, V. Delisser, S. Manaviazar, S. A. Peak, G. S. Bhatia, T. C. Collins, N. Jogiya, *Tetrahedron* **1996**, *52*, 1047–1068.
[15] J. H. Wu, R. Radinov, N. A. Porter, *J. Am. Chem. Soc.* **1995**, *117*, 11029–11030.
[16] M. P. Sibi, J. Ji, *J. Org. Chem.* **1996**, *61*, 6090–6091.
[17] M. P. Sibi, J. Ji, *J. Am. Chem. Soc.* **1996**, *118*, 9200–9201.
[18] Y. Yamamoto, S. Onuki, M. Yumoto, N. Asao, *J. Am. Chem. Soc.* **1994**, *116*, 421–422.
[19] C. L. Mero, N. A. Porter, *J. Am. Chem. Soc.* **1999**, *121*, 5155–5160.
[20] S. Caddick, S. Jenkins, *Tetrahedron Lett.* **1996**, *37*, 1301–1304.
[21] S. Caddick, S. Jenkins, N. Treweeke, S. X. Candeias, C. A. Afonso, *Tetrahedron Lett.* **1998**, *39*, 2203–2206.
[22] H. Kubota, A. Kubo, K. Nunami, *Tetrahedron Lett.* **1994**, *35*, 3107–3110.
[23] K. Nunami, H. Kubota, A. Kubo, *Tetrahedron Lett.* **1994**, *35*, 8639–8642.
[24] H. Kubota, A. Kubo, M. Takahashi, R. Shimizu, T.·Da-te, K. Okamura, K. Nunami, *J. Org. Chem.* **1995**, *60*, 6776–6784.
[25] A. Kubo, M. Takahashi, H. Kubota, K. Nunami, *Tetrahedron Lett.* **1995**, *36*, 6251–6252.
[26] A. Kubo, H. Kubota, M. Takahashi, K. Nunami, *Tetrahedron Lett.* **1996**, *37*, 4957–4960.
[27] A. Kubo, H. Kubota, M. Takahashi, K. Nunami, *J. Org. Chem.* **1997**, *62*, 5830–5837.
[28] S. Caddick, C. A. M. Afonso, S. X. Candeias, P. B. Hitchcock, K. Jenkins, L. Murtagh, D. Pardoe, A. G. Santos, N. R. Treweeke, R. Weaving, *Tetrahedron* **2001**, *57*, 6589–6605.
[29] A. G. Santos, S. X. Candeias, C. A. M. Afonso, K. Jenkins, S. Caddick, N. R. Treweeke, D. Pardoe, *Tetrahedron* **2001**, *57*, 6607–6614.
[30] A. G. Santos, J. Pereira, C. A. M. Afonso, G. Frenking, *Chem. Eur. J.* **2005**, *11*, 330–343.
[31] T. Poll, G. Helmchen, B. Bauer, *Tetrahedron Lett.* **1984**, *25*, 2191–2194.
[32] S. M. Bakalova, A. G. Santos, *J. Org. Chem.* **2004**, *69*, 8475–8481.
[33] T. Poll, J. O. Metter, G. Helmchen, *Angew. Chem.* **1985**, *97*, 116–118; *Angew. Chem. Int. Ed. Engl.* **1985**, *24*, 112–114.
[34] W. J. Hehre, L. Radom, P. v. R. Schleyer, J. A. Pople, *Ab initio MO Theory*, Wiley, New York, **1986**.
[35] W. Koch, M. C. Holthausen, *A Chemist's Guide to DFT*, 2nd ed., Wiley, New York, **2001**.
[36] L. Onsager, *J. Am. Chem. Soc.* **1938**, *58*, 1486–1493.
[37] S. Yamabe, T. Minato, *J. Org. Chem.* **2000**, *65*, 1830–1841.

[38] J. I. García, J. A. Mayoral, L. Salvatella, *Acc. Chem. Res.* **2000**, *33*, 658–664.
[39] M. J. Frisch, G. W. Trucks, H. B. Schlegel, G. E. Scuseria, M. A. Robb, J. R. Cheeseman, J. A. Montgomery Jr, T. Vreven, K. N. Kudin, J. C. Burant, J. M. Millam, S. S. Iyengar, J. Tomasi, V. Barone, B. Mennucci, M. Cossi, G. Scalmani, N. Rega, G. A. Petersson, H. Nakatsuji, M. Hada, M. Ehara, K. Toyota, R. Fukuda, J. Hasegawa, M. Ishida, T. Nakajima, Y. Honda, O. Kitao, H. Nakai, M. Klene, X. Li, J. E. Knox, H. P. Hratchian, J. B. Cross, C. Adamo, J. Jaramillo, R. Gomperts, R. E. Stratmann, O. Yazyev, A. J. Austin, R. Cammi, C. Pomelli, J. W. Ochterski, P. Y. Ayala, K. Morokuma, G. A. Voth, P. Salvador, J. J. Dannenberg, V. G. Zakrzewski, S. Dapprich, A. D. Daniels, M. C. Strain, O. Farkas, D. K. Malick, A. D. Rabuck, K. Raghavachari, J. B. Foresman, J. V. Ortiz, Q. Cui, A. G. Baboul, S. Clifford, J. Cioslowski, B. B. Stefanov, G. Liu, A. Liashenko, P. Piskorz, I. Komaromi, R. L. Martin, D. J. Fox, T. Keith, M. A. Al-Laham, C. Y. Peng, A. Nanayakkara, M. Challacombe, P. M. W. Gill, B. Johnson, W. Chen, M. W. Wong, C. Gonzalez, J. A. Pople, *Gaussian 03*, *Revision B.05*, Gaussian, Inc., Pittsburgh PA, **2003**.
[40] C. González, H. B. Schlegel, *J. Chem. Phys.* **1989**, *90*, 2154–2161.
[41] S. Kong, J. D. Evanseck, *J. Am. Chem. Soc.* **2000**, *122*, 10418–10427.
[42] D. M. Birney, K. N. Houk, *J. Am. Chem. Soc.* **1990**, *112*, 4127–4133.
[43] J. I. García, V. Martínez-Merino, J. A. Mayoral, L. Salvatella, *J. Am. Chem. Soc.* **1998**, *120*, 2415–2420.
[44] O. Acevedo, J. D. Evanseck, *Org. Lett.* **2003**, *5*, 649–652.
[45] R. J. Loncharich, T. R. Schwartz, K. N. Houk, *J. Am. Chem. Soc.* **1987**, *109*, 14–23.
[46] A. Virdi, V. P. Gupta, A. Sharma, *J. Mol. Struct. (THEOCHEM)* **2003**, *634*, 53–65.
[47] A. Sbai, V. Branchadell, R. M. Ortuño, A. Oliva, *J. Org. Chem.* **1997**, *62*, 3049–3054.
[48] D. A. Singleton, S. R. Merrigan, B. R. Beno, K. N. Houk, *Tetrahedron Lett.* **1999**, *40*, 5817–5821.
[49] J. I. García, J. A. Mayoral, L. Salvatela, *Eur. J. Org. Chem.* **2005**, 85–90.
[50] J. I. Garcia, J. A. Mayoral, L. Salvatela, *Tetrahedron* **1997**, *53*, 6057–6064.
[51] D. A. Evans, B. D. Allison, M. G. Yang, *Tetrahedron Lett.* **1999**, *40*, 4457–4460.
[52] D. A. Evans, B. D. Allison, M. G. Yang, C. E. Masse, *J. Am. Chem. Soc.* **2001**, *123*, 10840–10852.
[53] D. A. Evans, K. A. Scheidt, J. N. Johnston, M. C. Willis, *J. Am. Chem. Soc.* **2001**, *123*, 4480–4491.

Received: October 16, 2005
Published Online: January 31, 2006

